

SIRUP: A DIFFUSION-BASED VIRTUAL UPMIXER OF STEERING VECTORS FOR HIGHLY-DIRECTIVE SPATIALIZATION WITH FIRST-ORDER AMBISONICS

Emilio Picard^{1,2} Diego Di Carlo¹ Aditya Arie Nugraha¹ Mathieu Fontaine^{3,1} Kazuyoshi Yoshii^{4,1}

¹Center for Advanced Intelligence Project, RIKEN, Japan

²Sorbonne University, France

³LTCI, Télécom Paris, Institut Polytechnique de Paris, France

⁴Graduate School of Engineering, Kyoto University, Japan

ABSTRACT

This paper presents virtual upmixing of steering vectors captured by a fewer-channel spherical microphone array. This challenge has conventionally been addressed by recovering the directions and signals of sound sources from first-order ambisonics (FOA) data, and then rendering the higher-order ambisonics (HOA) data using a physics-based acoustic simulator. This approach, however, struggles to handle the mutual dependency between the spatial directivity of source estimation and the spatial resolution of FOA ambisonics data. Our method, named SIRUP, employs a latent diffusion model architecture. Specifically, a variational autoencoder (VAE) is used to learn a compact encoding of the HOA data in a latent space and a diffusion model is then trained to generate the HOA embeddings, conditioned by the FOA data. Experimental results showed that SIRUP achieved a significant improvement compared to FOA systems for steering vector upmixing, source localization, and speech denoising.

Index Terms— Steering vectors, virtual upmixing, latent diffusion model, sound source localization, beamforming.

1. INTRODUCTION

Sound source localization (SSL) and speech enhancement (SE) or denoising remain fundamental tasks in machine listening applications, further used in augmented reality (AR) scenes [1], as well as robotics [2], radar [3], and autonomous driving systems [4]. Beamforming and SSL methods are still widely characterized by acoustic and signal processing [5–7], even though recent work tried to incorporate deep neural networks (DNNs) to address such tasks [8, 9]. These applications call for more accurate spatial information that could be translated as more selective beam patterns, enabling better localization and spatial filtering.

High-order-ambisonic (HOA) microphone arrays [10] are capable of high spatial resolutions, enabling effective sound

This work was supported by JST FOREST no. JPMJFR2270, JSPS KAKENHI nos. JP23K16912, JP23K16913, 24H00742, 24H00748, and 25H01142, and ANR Project SAROUMANE (ANR-22-CE23-0011). All the code used to produce the results of this paper is available at <https://github.com/emilio-pcrd/sirup> upon acceptance.

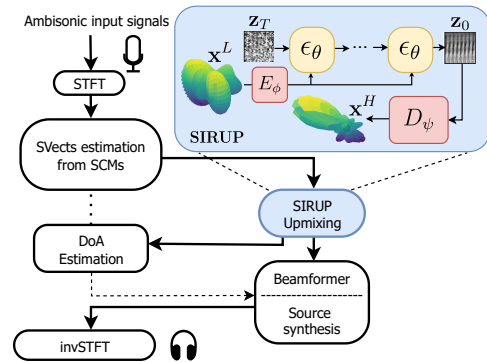


Fig. 1: The SIRUP upmixer for downstream tasks.

analysis and synthesis [11, 12]. The spatial resolution of these systems does relate to the number of ambisonic orders, which are related to the number of microphones. These limitations can be alleviated by adopting HOA setup, albeit at the expense of expensive hardware; consequently, common spatial recording systems are typically constrained to the first order (FOA), employing four microphones.

A common remedy is parametric *upmixing*, which estimates scene parameters, e.g., directions of arrival (DOA) via SSL and source signals via separation or SE, and then render virtual HOA channels. For example, major methods such as DirAC [13] and COMPASS [14] encode directional and ambient components before ad-hoc HOA spatial rendering [15]. Their performance is tightly coupled to the accuracy of steering vectors (SVs), the spatial signatures driving classical SSL (e.g., SRP-PHAT) and SE (e.g., delay-and-sum beamforming) [16]. This cascaded analysis–rendering pipeline is brittle: low-resolution noisy FOA SVs degrade the parameter estimates and propagate errors to the HOA rendering.

We instead propose to directly upmix the *ambisonic SVs*. SVs compactly encode the spatial characteristics of sources, encompassing both the direct paths and early reflections. By super-resolving FOA SVs, one can perform SSL in a highly-directive HOA space, allowing the DOA estimates to produce sharper spatial filters. The upmixed SVs can also be utilized to render the source images at a higher spatial resolution.

Specifically, a SteerIng vector UPmixer (SIRUP) learns a latent space of HOA SVs with a VAE and uses a conditional diffusion model to generate HOA embeddings from FOA inputs estimated under an isotropic ambient prior. Once DOAs are inferred from the reconstructed HOA SVs, source signals are recovered via beamforming and subsequently rendered using FOA-consistent or either algebraic free-field SVs, as depicted in Fig. 1.

2. BACKGROUND

This section introduces SVs and their applications. We work in the short-time Fourier transform (STFT) domain whose frequency bins and time frames are indexed with $f \in \{1, \dots, F\}$ and $t \in \{1, \dots, T\}$, where F and T are the numbers of frequency bins and frames, respectively.

2.1. Steering vectors

Suppose we have an M -channel STFT observation $\mathbf{x}_{ft} \in \mathbb{C}^M$ of a static, far-field source [6], which is given by

$$\mathbf{x}_{ft} = \mathbf{a}_f s_{ft} + \mathbf{n}_{ft}, \quad (1)$$

where $\mathbf{a}_f \in \mathbb{C}^M$ is the acoustic transfer function, $s_{ft} \in \mathbb{C}$ the source STFT, and $\mathbf{n}_{ft} \in \mathbb{C}^M$ diffuse isotropic noise.

For a given array geometry and look direction θ , the algebraic SVs that models the direct path of \mathbf{a}_f is [6]

$$\tilde{\mathbf{a}}_f(\theta) = [e^{-j2\pi f \tau_1(\theta)}, \dots, e^{-j2\pi f \tau_M(\theta)}]^\top, \quad (2)$$

with relative delays $\tau_m(\theta) = \mathbf{u}_\theta^\top (\mathbf{r}_m - \bar{\mathbf{r}})/c$, where \mathbf{r}_m is the m -th microphone position, $\bar{\mathbf{r}}$ the array center, \mathbf{u}_θ the unit vector pointing to θ , and c the speed of sound.

The dominant spatial mode of the spatial covariance matrix (SCM) provides a good estimate of the SVs [17]:

$$\hat{\Sigma}_f = \frac{1}{T} \sum_{t=1}^T \mathbf{x}_{ft} \mathbf{x}_{ft}^H, \quad \hat{\mathbf{a}}_f = \text{eig}_1(\hat{\Sigma}_f), \quad (3)$$

where $\text{eig}_1(\cdot)$ denotes the principal eigenvector. These measured SVs capture the direct path plus early reflections, and thus are richer than the algebraic model in Eq. (2).

2.2. Applications

For SSL, we evaluate the steered-response-power (SRP) map on a discrete grid of DOAs and pick one $\hat{\theta}$ [18] as follows:

$$\mathcal{S}(\theta) = \sum_f \left| \frac{\tilde{\mathbf{a}}_f(\theta)^H \hat{\mathbf{a}}_f}{\|\tilde{\mathbf{a}}_f(\theta)\|_2 \|\hat{\mathbf{a}}_f\|_2} \right|^2, \quad \hat{\theta} = \arg \max_{\theta} \mathcal{S}(\theta). \quad (4)$$

This corresponds to cross-correlation between the estimated SV and algebraic SVs computed in the frequency domain.

For SE, a beamformer steered to $\hat{\theta}$ is given by

$$\mathbf{w}_f = \frac{\mathbf{a}_f(\hat{\theta})}{\|\mathbf{a}_f(\hat{\theta})\|_2}, \quad \hat{s}_{ft} = \mathbf{w}_f^H \mathbf{x}_{ft}, \quad (5)$$

where \mathbf{a}_f can be either the algebraic or measured SV pointing at $\hat{\theta}$ direction. Assuming spatially white noise, choosing

$\mathbf{w}_f \propto \hat{\mathbf{a}}_f$ yields the MaxSINR beamformer [19].

2.3. Latent diffusion models for image out-painting

Given a cropped image $\mathbf{x}^L \in \mathbb{R}^{I_L \times J_L}$, *out-painting* aims at recovering the missing regions of an original image $\mathbf{x}^H \in \mathbb{R}^{I_H \times J_H}$ with $I_H > I_L, J_H > J_L$. This approach naturally extends for audio super-resolution [20]. State-of-the-art performances on these tasks are obtained with latent diffusion models [21–24], where the diffusion is processed in a latent space learned by a variational autoencoder (VAE).

Let E_ϕ and D_ψ be the VAE encoder and decoder, i.e. $\mathbf{z}_0 = E_\phi(\mathbf{x}^H), \hat{\mathbf{x}}^H = D_\psi(\mathbf{z}_0)$. In diffusion models, the forward process represents the variational posterior $q(\mathbf{z}_{1:T}|\mathbf{z}_0)$ as a Gaussian Markov chain, where noise is gradually added to the latent vector \mathbf{z}_0 according to a fixed schedule. In latent diffusion, the reverse process $p_\theta(\mathbf{z}_{0:T}|\mathbf{c})$ is similarly modeled as a Gaussian Markov chain, conditioned on a context embedding $\mathbf{c} = \mathcal{C}(\mathbf{x}^L)$ injected via concatenation or cross-attention into the denoising network $\epsilon_\theta(\mathbf{z}_t, t, \mathbf{c})$. The function ϵ_θ is used to predict the mean of each $p_\theta(\mathbf{z}_{t-1}|\mathbf{z}_t, \mathbf{c})$. The training score is $\mathbb{E}[\|\epsilon - \epsilon_\theta(\mathbf{z}_t, t, \mathbf{c})\|^2]$ where $\epsilon \sim \mathcal{N}(\mathbf{0}, \mathbf{I})$ and \mathbf{z}_t is a linear combination of \mathbf{z}_0 and ϵ .

3. PROPOSED METHOD

This section introduces the proposed SV upmixing method that extends a latent diffusion models to SV spatial super-resolution, and discuss its application for audio analysis.

3.1. Steering vector upmixing

The proposed SIRUP model is a conditioned latent diffusion model that uses the first M channels to generate the missing $M' - M$ ambisonic channels, yielding the upmixed SVs $\hat{\mathbf{A}}^{\text{up}} \in \mathbb{C}^{F \times M'}$ with $M' > M$. Let $\hat{\mathbf{A}} \in \mathbb{C}^{F \times M}$ be the concatenation of measured FOA SVs across frequency and define the conditioning tensor by zero-padding channels as

$$\mathbf{c} = [\hat{\mathbf{A}}, \mathbf{0}_{F \times (M' - M)}] \in \mathbb{C}^{F \times M'}. \quad (6)$$

Optionally, the algebraic SVs may fill $\mathbf{c}_{:,M+1:M'}$ if steering directions are known.

Then we encode the condition with a VAE encoder E_ϕ and run latent diffusion conditioned on this embedding. Starting from pure noise $\mathbf{z}_T \sim \mathcal{N}(\mathbf{0}, \mathbf{I})$, the denoiser $\epsilon_\theta(\mathbf{z}_t, t, E_\phi(\mathbf{c}))$ iteratively produces \mathbf{z}_{t-1} until \mathbf{z}_0 . The decoder D_ψ then produces the super-resolved ambisonic SVs:

$$\mathbf{z}_{t-1} = \epsilon_\theta(\mathbf{z}_t, t; E_\phi(\mathbf{c})), \quad \hat{\mathbf{A}}^{\text{up}} = D_\psi(\mathbf{z}_0). \quad (7)$$

During inference, the latent diffusion model is used to sample from pure noise and the condition, to generate a suitable latent candidate for the decoder. The VAE thus acts as a training-time regularizer establishing a well-behaved latent manifold, through a small KL-divergence penalty.

To enhance spatial reconstruction, we employ a composited loss function that combines a cosine similarity term with

both feature-matching and mean squared error (MSE) objectives. This significantly improves both learning stability and overall performance. Furthermore, dilated convolutions are introduced along the frequency axis of the network architecture. This modification enforces spatial coherence across different frequency bands, while the microphone axis coherence is already implicitly handled by the cosine similarity term.

3.2. Downstream tasks with up-mixed steering vectors

Figure 1 outlines the proposed upmixing pipeline for sound-scene analysis and synthesis. First, measured SVs $\hat{\mathbf{a}}_f \in \mathbb{C}^M$ for the target source are estimated from the multichannel mixture $\mathbf{x}_{ft} \in \mathbb{C}^M$ over a short time window using Eq. (3). Next, the M -channel ambisonic representation of $\hat{\mathbf{a}}_f$ is upmixed to a higher ambisonic order with M' channels via SIRUP (cf. Section 3.1), and then mapped back to the signal domain as SVs of a virtual M' -channel spherical array.

SSL is subsequently performed in the upmixed domain using Eq. (4) as a grid search using algebraic SVs projected onto the upmixed counterparts. For enhancement and rendering, the upmixed SVs can be truncated to the original M -channel subspace to obtain denoised spatial images. Note that SIRUP can also be trained with a denoising objective to refine the first M ambisonic coefficients, thereby improving the accuracy of the estimated SVs.

4. EVALUATION

This section presents the performance of the proposed upmixing approach in terms of SSL and beamforming metrics.

4.1. Experimental settings

We first explain the experimental data, model configuration, and evaluation metrics.

4.1.1. Experimental data

Room impulse responses (RIRs) were simulated using the image source model (ISM) in the `pyroomacoustics` library [25]. For each investigation, we generated 30 distinct acoustic scenes with various signal-to-noise ratios (\mathcal{D}_{SNR}) and reverberation times ($\mathcal{D}_{\text{RT60}}$). The microphone array was centrally placed in a $6 \times 4 \times 3$ m room, with its horizontal position randomized by up to 1 m. Source locations were randomly selected within the azimuth plane, with a fixed elevation of approximately 28° . This specific elevation was chosen to simulate a typical desktop condition, where the microphones are placed on top of a table. All sources were modeled as point speech sources, randomly selected and cropped to 4 seconds from the *dev-clean* folder of the *LibriSpeech* database [26].

For SSL experiments and testing the upmixing method, we simulated rooms containing a single speech source with reverberation and noise. The SVs were directly estimated from the mixture using Eq. (3). For SE experiments, we simulated mixtures comprising two speech sources across various

acoustic environments. To compute their SVs, we introduced a 2-second delay between the start times of the two 4-second sources. This configuration allowed us to use the first 2 seconds and the last 2 seconds of the overall mixture for the SV estimation of the first and second sources, respectively.

All data were sampled at $f_s = 16$ kHz. The short-time Fourier transform (STFT) was computed using a 512-sample frame size with 50% overlap and a Hamming window. For the ambisonic representation, third-order data ($M' = 16$) were designated as the target HOA data, corresponding to first-order ambisonics ($M = 4$) as the low-resolution input.

4.1.2. Model configuration

The training of SIRUP was conducted in a two-stage process. In the first stage, a VAE was trained to reconstruct HOA SVs conditioned on FOA SVs. The training data consisted of measured SVs obtained from single-source noisy mixtures utilizing Eq. (3). The autoencoder (3.1M parameters) was optimized for 40 epochs using the AdamW optimizer with a learning rate of 3×10^{-4} . The objective function (Section 3) combined an ℓ_2 reconstruction loss, a cosine loss objective, a perceptual loss, and a small KL term.

The second stage involved freezing the encoder and fine-tuning only the decoder for an additional 20 epochs. This fine-tuning utilized a combination of MSE and cosine similarity losses, applied with an exponential learning-rate schedule. We trained a UNet-based latent diffusion model (4.1M parameters) as in [24]. This model operates within the VAE latent space to perform the upmixing task, conditioned on the FOA inputs. Prior to inputting the latent values to the UNet, the encoder outputs were scaled to the range $[-1, 1]$ [24].

Conditions were injected into the UNet in two ways: (i) concatenation of the FOA tensor with the noisy latent representation at the UNet input layer and (ii) application of cross-attention within each architectural block. Training was conducted for 100 epochs with AdamW at a learning rate of 3×10^{-4} . The total number of diffusion steps, T , was set to 1,000 during training and 200 during inference.

For training, 3,000 pairs of measured FOA and HOA SVs ($\hat{\mathbf{A}} \in \mathbb{C}^{F \times M}$, $\hat{\mathbf{a}}^{\text{up}} \in \mathbb{C}^{F \times M'}$) were used. The target HOA data were generated by convolving the source signals with the simulated RIRs. The corresponding FOA data were obtained by retaining only the first $M = 4$ channels of the HOA data. We represent complex SVs as stacked real/imag parts, hence the leading dimension “2” in tensors of shape $(2, F, M)$ and $(2, F, M')$, respectively. The remaining $(M' - M)$ channels required for the model input were addressed by zero-padding the FOA conditioning tensor.

4.1.3. Evaluation metrics

To assess performance, we utilized two distinct evaluation sets: \mathcal{D}_{SNR} and $\mathcal{D}_{\text{RT60}}$. In the \mathcal{D}_{SNR} set, the SNR was varied within the range $[5, 20]$ dB while the reverberation time was fixed at $\text{RT60} = 0.2$ s. Conversely, in the $\mathcal{D}_{\text{RT60}}$ set, RT60 was varied within $[0.2, 0.7]$ s with a fixed $\text{SNR} = 20$ dB.

Table 1: Performances for different spatial representations, averaged over 30 simulated rooms. Ground-truth HOA values (gray) are provided for reference. Beamwidth is measured at -3dB (lower is better).

	DI [dB] \uparrow			3-dB BW [$^\circ$] \downarrow			SL [dB] \downarrow		
	FOA	Upmixed	HOA	FOA	Upmixed	HOA	FOA	Upmixed	HOA
\mathcal{D}_{RT60}	10.0 \pm 2.6	19.8 \pm 2.3	20.0 \pm 2.2	30 \pm 6	24.0 \pm 3.3	24 \pm 2	-0.9 \pm 0.7	-9.5 \pm 3.1	-11.2 \pm 2.8
\mathcal{D}_{SNR}	8.1 \pm 2.7	17.1 \pm 2.1	17.7 \pm 2.0	48.0 \pm 6.7	27.0 \pm 3.5	26.0 \pm 2.2	-1.2 \pm 0.9	-9.6 \pm 3.4	-11.7 \pm 2.7

Table 2: Source synthesis enhancement from mixture across varying for mixtures of two speech sources.

Metric	Measured SVs		Algebraic SVs following SSL	
	SV-FOA	SV-SIRUP-M	SV-alg FOA	SV-alg SIRUP
SDR [dB]	17.2 \pm 3.2	17.4 \pm 3.1	12.6 \pm 7.4	13.0 \pm 7.2
SIR [dB]	38.8 \pm 3.6	38.8 \pm 3.3	33.5 \pm 7.8	34.0 \pm 7.5
SAR [dB]	17.3 \pm 3.2	17.4 \pm 3.1	12.6 \pm 7.3	13.0 \pm 7.2

SSL performance was primarily evaluated in terms of the angular error on the azimuthal plane, benchmarked against an SRP baseline derived from FOA mixtures. To assess the quality of the upsampled SVs, we considered the directivity index (DI), the 3dB-beamwidth (3dB BW), and sidelobe (SL) metrics. Finally, the output of the beamforming process was evaluated using common source separation metrics, as detailed in Tab. 2 and computed using the `bss_eval` toolkit [6].

4.2. Experimental results

Fig. 2 reports the average DOA estimation error of the sound source by pickpeaking on the SRP angular map (shown in Fig 3, against different noise and reverberation ratios. SIRUP was shown to have outperformed the FOA in noisy conditions, begin closed to the topline using HOA setup. We however reports comparable results increasing the reverberation.

Next, we investigate the spatial quality of the upmixed SVs compared to the FOA baseline in terms of beampattern metrics computed azimuthal plane. As reported in Table 1, the proposed method SIRUP yields an average beamwidth improvement of $+10^\circ$ and sidelobes suppression of -9 dB. Qualitatively, this performances translate in narrower beam shapes comparable to the one of a HOA setup, as shown in 3.

Finally, we studied the beamforming performance for mixtures of 2 sources. The results reported in Table 2 compare the denoised output when using the following SVs model for beamforming as in Eq. (5): the SVs compute for FOA mixture (SV-FOA), the first M channels of the SIRUP’s output (SV-SIRUP-M), the algebraic SVs from DOA estimation of both the measured FOA SVs (SV-alg FOA) and SIRUP (SV-alg SIRUP), respectively. The performances of SV-SIRUP-M are expected to be comparable the one of SV-FOA denoting effective training of the diffusion model. However, we observed improvements, which can be explained by the capacity of the model to denoise SVs during inference. In addition, as we have better DOA estimation using SIRUP, we also note

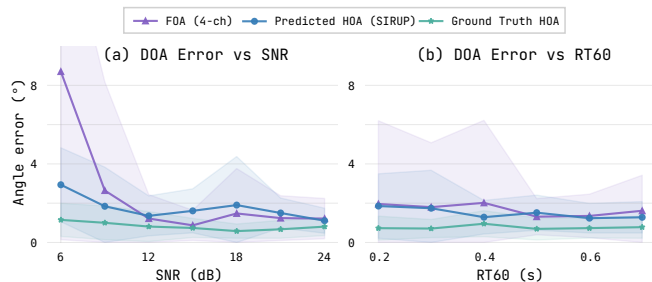


Fig. 2: Average angular errors across conditions using different localization methods and SV models, using SRP (Eq. (5)).

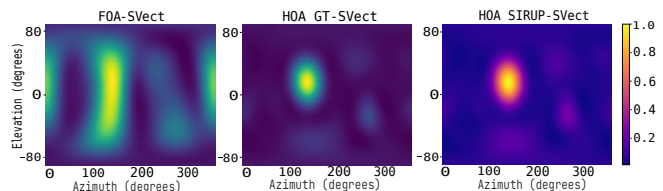


Fig. 3: 2D Heatmap comparison of estimated SV for FOA and ground truth HOA setup.

improvements for the SV-alg experiments. In most practical cases, SIRUP is outperforming the FOA conditions with equal information, leading to spatial-resolution improvements in every experiences.

5. CONCLUSION

This paper presented a novel diffusion-based approach named SIRUP, designed to significantly enhance the spatial information derived from FOA setups, allowing it to emulate the performance of HOA microphone arrays. SIRUP directly addresses the inherent limitations of FOA systems, such as lower spatial resolution and imprecise SSL, by virtually upmixing SVs using a two-step latent diffusion model. The experimental results demonstrated that SIRUP achieved significant improvements in steering vector upmixing, sound source localization, and speech denoising compared to FOA systems.

Future work will focus on comprehensively utilizing the upmixed SVs for downstream tasks like source separation and rendering. We also plan to make the model capable of learning from noisier SVs. These advancements could significantly enhance machine listening applications requiring high spatial accuracy, such such as augmented reality, robotics, radar, and autonomous driving systems.

6. REFERENCES

- [1] R. Gupta, J. He, R. Ranjan, W.-S. Gan, F. Klein, C. Schneiderwind, A. Neidhardt, K. Brandenburg, and V. Välimäki, “Augmented/mixed reality audio for hearables: Sensing, control, and rendering,” *IEEE Signal Processing Magazine*, vol. 39, no. 3, pp. 63–89, 2022.
- [2] J. Wang, Y. He, D. Su, K. Itoyama, K. Nakadai, J. Wu, S. Huang, Y. Li, and H. Kong, “Slam-based joint calibration of multiple asynchronous microphone arrays and sound source localization,” *IEEE Transactions on Robotics*, vol. 40, pp. 4024–4044, 2024.
- [3] P. Barton, “Digital beam forming for radar,” *IEEE Proc. of Communications, Radar and Signal Processing*, vol. 127, no. 4, pp. 266–277, 1980.
- [4] I. Marques, J. Sousa, B. Sá, D. Costa, P. Sousa, S. Pereira, A. Santos, C. Lima, N. Hammerschmidt, S. Pinto, and T. Gomes, “Microphone array for speaker localization and identification in shared autonomous vehicles,” *Electronics*, vol. 11, no. 5, pp. 766, 2022.
- [5] J. H. DiBiase, *A high-accuracy, low-latency technique for talker localization in reverberant environments using microphone arrays*, Ph.D. thesis, Brown University, 2000.
- [6] E. Vincent, T. Virtanen, and S. Gannot, *Audio Source Separation and Speech Enhancement*, Wiley, 1st edition, 2018.
- [7] R. Schmidt, “Multiple emitter location and signal parameter estimation,” *IEEE Trans. on Antennas and Propagation*, vol. 34, no. 3, pp. 276–280, 1986.
- [8] S. Adavanne, A. Politis, and T. Virtanen, “Differentiable tracking-based training of deep learning sound source localizers,” in *Proc. WASPAA. IEEE*, 2021, pp. 211–215.
- [9] S. Adavanne, A. Politis, J. Nikunen, and T. Virtanen, “Sound event localization and detection of overlapping sources using convolutional recurrent neural networks,” *IEEE Journal of Selected Topics in Signal Processing*, vol. 13, no. 1, pp. 34–48, 2019.
- [10] M. Poletti, “Three-dimensional surround sound systems based on spherical harmonics,” *Journal of the Audio Engineering Society*, 2012.
- [11] S. Bertet, J. Daniel, E. Parizet, and O. Warusfel, “Investigation on localisation accuracy for first and higher order ambisonics reproduced sound sources,” *Acta Acustica united with Acustica*, vol. 99, pp. 642 – 657, 07 2013.
- [12] A. Avni, J. Ahrens, M. Geier, S. Spors, H. Wierstorf, and B. Rafaely, “Spatial perception of sound fields recorded by spherical microphone arrays with varying spatial resolution,” *The Journal of the Acoustical Society of America*, vol. 133, no. 5, pp. 2711–2721, May 2013.
- [13] G. Fuchs, F. Ghido, D. Weckbecker, and O. Thiergart, “A first-order dirac-based parametric ambisonic coder for immersive communications,” in *Proc. ICASSP*, 2025, pp. 1–5.
- [14] A. Politis, S. Tervo, and V. Pulkki, “Compass: Coding and multidirectional parameterization of ambisonic sound scenes,” in *Proc. ICASSP*, 2018, pp. 6802–6806.
- [15] D. P. Jarrett, E. A. Habets, M. R. Thomas, and P. A. Naylor, “Rigid sphere room impulse response simulation: Algorithm and applications,” *The Journal of the Acoustical Society of America*, vol. 132, no. 3, pp. 1462–1472, 2012.
- [16] S. Gannot, E. Vincent, S. Markovich-Golan, and A. Ozerov, “A consolidated perspective on multimicrophone speech enhancement and source separation,” *IEEE/ACM Trans. on Audio, Speech, and Lang. Process.*, vol. 25, no. 4, pp. 692–730, 2017.
- [17] S. Markovich, S. Gannot, and I. Cohen, “Multichannel eigenspace beamforming in a reverberant noisy environment with multiple interfering speech signals,” *IEEE Trans. on Audio, Speech, and Language Processing*, vol. 17, no. 6, pp. 1071–1086, 2009.
- [18] E. Grinstein, E. Tengan, B. Çakmak, T. Dietzen, L. Nunes, T. van Waterschoot, M. Brookes, and P. A. Naylor, “Steered response power for sound source localization: A tutorial review,” *EURASIP Journal on Audio, Speech, and Music Processing*, vol. 2024, no. 1, pp. 59, 2024.
- [19] J. Kim and C.-K. Un, “Signal subspace method for beam-steered adaptive arrays,” *Electronics Letters*, vol. 25, no. 16, pp. 1076–1077, 1989.
- [20] H. Liu, K. Chen, Q. Tian, W. Wang, and M. D. Plumbley, “Audios: Versatile audio super-resolution at scale,” 2023.
- [21] Q. Xiao, G. Li, and Q. Chen, “Image outpainting: Hallucinating beyond the image,” *IEEE Access*, vol. 8, pp. 173576–173583, 2020.
- [22] R. Rombach, A. Blattmann, D. Lorenz, P. Esser, and B. Ommer, “High-resolution image synthesis with latent diffusion models,” *Proc. CVPR*, 2022.
- [23] J. Ho, A. Jain, and P. Abbeel, “Denoising diffusion probabilistic models,” *Advances in Neural Information Processing Systems*, 2020.
- [24] Z. Evans, C. Carr, J. Taylor, S. H. Hawley, and J. Pons, “Fast timing-conditioned latent audio diffusion,” in *Int. Conf. on Machine Learning*, 2024.
- [25] R. Scheibler, E. Bezzam, and I. Dokmanic, “Pyroomacoustics: A python package for audio room simulation and array processing algorithms,” in *Proc. ICASSP*, 2018, pp. 351–355.
- [26] V. Panayotov, G. Chen, D. Povey, and S. Khudanpur, “Librispeech: An asr corpus based on public domain audio books,” in *Proc. ICASSP*, 2015, pp. 5206–5210.